Computers and Geosciences 109 (2017) 16–24

Contents lists available at ScienceDirect

Computers and Geosciences

journal homepage: www.elsevier.com/locate/cageo

Research paper

Guided SAR image despeckling with probabilistic non local weights

Jithin Gokul [a], Madhu S. Nair [b], Jeny Rajan [a,*]

[a] Department of Computer Science and Engineering, National Institute of Technology Karnataka, Surathkal, India
[b] Department of Computer Science, University of Kerala, Kariavattom, Thiruvananthapuram, India

ARTICLE INFO

Keywords:
SAR imaging
Speckle
Denoising
Non-local means
Guided filtering

ABSTRACT

SAR images are generally corrupted by granular disturbances called speckle, which makes visual analysis and detail extraction a difficult task. Non Local despeckling techniques with probabilistic similarity has been a recent trend in SAR despeckling. To achieve effective speckle suppression without compromising detail preservation, we propose an improvement for the existing Generalized Guided Filter with Bayesian Non-Local Means (GGF-BNLM) method. The proposed method (Guided SAR Image Despeckling with Probabilistic Non Local Weights) replaces parametric constants based on heuristics in GGF-BNLM method with dynamically derived values based on the image statistics for weight computation. Proposed changes make GGF-BNLM method adaptive and as a result, significant improvement is achieved in terms of performance. Experimental analysis on SAR images shows excellent speckle reduction without compromising feature preservation when compared to GGF-BNLM method. Results are also compared with other state-of-the-art and classic SAR depseckling techniques to demonstrate the effectiveness of the proposed method.

1. Introduction

Synthetic Aperture Radar applications include aerial surveillance using high-resolution imaging, sub surface imaging for mineral estimation, oceanography, climatic studies, space science and defense. SAR imaging being coherent in nature (Moreira et al., 2013), is affected by granular disturbances called speckle, which follows multiplicative model (Frost et al., 1982). Echoed radar waves go out of phase randomly for the same target region and, these signals when combined interferes constructively or destructively to form speckle (Argenti et al., 2013). Presence of speckle makes visual analysis and detail extraction from SAR images a difficult task and hence despeckling is a fundamental step in SAR image processing. Fine details and edge information in the image should also be preserved during the despeckling process.

Numerous SAR despeckling techniques have been proposed in the last three decades. Lee filter (Lee, 1980) is a classic technique in despeckling which makes use of the local statistics within the noisy image. Minimum Mean Square Error (MMSE) estimation is then applied to estimate the noise free pixel values. Kuan (Kuan et al., 1985), Frost (Frost et al., 1982) and Gamma MAP (Lopes et al., 1990a) filters also belong to this category of spatial adaptive filters which employs MMSE estimation. Lopes et al. (1990b). proposed an improved adaptive filter which makes use of scene heterogeneity for edge preservation. Apart from spatial domain filters, several despeckling techniques have been proposed in the wavelet domain also. Filtering in the wavelet domain involves inter-domain transform of the original image with Discrete Wavelet Transform (DWT), Undecimated Discrete Wavelet Transform (UDWT) (Argenti et al., 2013) or other similar techniques. Noise free wavelet coefficients are then estimated followed by the inverse transform to the original domain to generate the denoised image. Speckle filters in wavelet domain can preserve edges with appropriate thresholding techniques, but they may introduce ring like artifacts (Bianchi et al., 2008; Tao et al., 2012).

Buades et al. (2005). proposed a Non Local Means (NLM) method in 2005 in which the true underlying intensity is estimated by computing the weighted average of non local pixels within the image. NLM gave excellent results for Additive White Gaussian Noise (AWGN). Several modifications were proposed for NLM which includes - adaptive selection of the search region, early termination of similarity check and introduction of new similarity measures (Jojy et al., 2013). Bayesian Non Local Means (BNLM) (Coupe et al., 2008) originally proposed for Ultrasound despeckling adapted the NLM concept to denoise multiplicative speckle using Bayesian framework. In Zhong et al. (2009), a new similarity measure based on likelihood is adopted and applied Bayesian Non Local Means concept to SAR despeckling. An iteratively refined despeckling based on the noise model which uses maximum likelihood

* Corresponding author.
E-mail address: jenyrajan@gmail.com (J. Rajan).

http://dx.doi.org/10.1016/j.cageo.2017.07.004
Received 27 December 2016; Received in revised form 17 May 2017; Accepted 13 July 2017
Available online 21 July 2017
0098-3004/© 2017 Elsevier Ltd. All rights reserved.

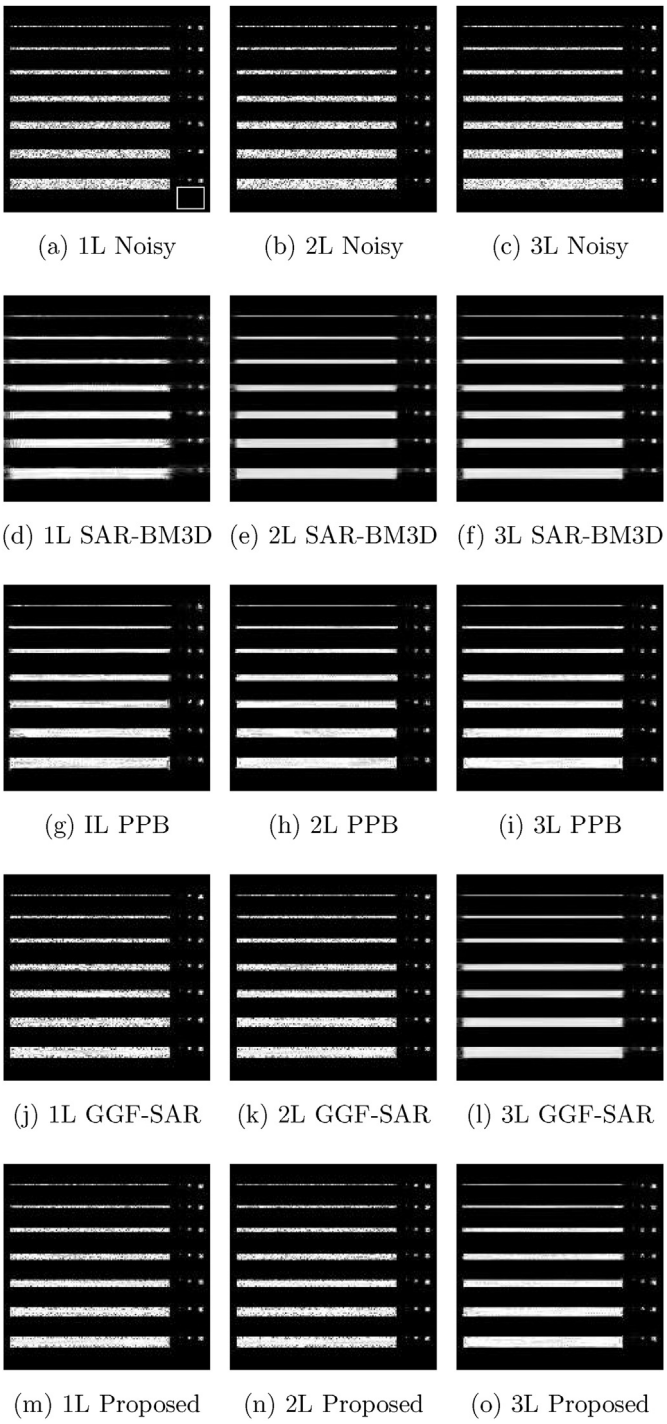

Fig. 1. Comparison of proposed method against SAR-BM3D, PPB and GGF-BNLM for phantom image.

estimation technique was proposed in Deledalle et al. (2009). This iterative Maximum Likelihood denoising with probabilistic weights give excellent speckle suppression in homogeneous regions, but fails to preserve sharp details in images with high noise level (Ni and Gao, 2016).

He et al. (2013) introduced the concept of guided image filtering (He et al., 2013) for AWGN, which filters the input image with the aid of a guidance image. Guidance image can be the same noisy input image or an explicit one. A linear relationship between the noisy image and guidance image is assumed and the guidance image guides the structure transferring filter operation. In Verdoliva et al. (2014),(2015), co-registered optical guidance image of the same target scene were used for guided SAR despeckling. These techniques require an optical image of the same target region to despeckle the SAR image which is a severe restriction. Generalized Guided Filter with Bayesian Non Local Means (GGF-BNLM) (Ni and Gao, 2016) used guided filtering to derive the priori component within probabilistic patch based weights discussed in Deledalle et al. (2009) for the despeckling of SAR images. In GGF-BNLM, the relative contribution of likelihood and priori components in estimating the probabilistic weights is determined by coefficients whose values are derived based on heuristics.

In this paper, we propose an improvement for the GGF-BNLM method by replacing the coefficients based on heuristics with dynamically derived weights based on local image statistics. The relative contribution of priori component in weight estimation is decided by the degree of variance within the local patches. This adaptive approach helps in preserving the edges in a better way. We also replaced the coefficient of likelihood component based on heuristics with the normalization parameter discussed in Deledalle et al. (2009). As a second improvement, we replaced the adaptive filtering based on Maximum-Likelihood rule with more detail preserving MMSE estimation technique to estimate the guidance image. With the above modifications in place, the proposed method performs better in terms of smoothing and detail preservation than the conventional GGF-BNLM method. Results are also compared with other state-of-the-art filters which includes PPB (Deledalle et al., 2009), BNLM-SAR (Zhong et al., 2009) and SAR-BM3D (Parrilli et al., 2012) to demonstrate the effectiveness of the proposed method.

Remaining sections of the paper are organized as follows. Section 2 discusses the noise characteristics of SAR images. Section 3 contains a detailed analysis of GGF-BNLM method highlighting the drawbacks and the scope of improvement. In Section 4 we introduce the proposed method. Experimental results and comparative analysis are included in Section 5. Concluding remarks are drawn in Section 6.

2. Noise characteristics in SAR images

If there are no point scatterers (Moreira et al., 2013) in the target resolution cell, back scattered echoes from the same region will have approximately the same reflectivity levels. They can be represented as collective sum of individual back-scattered echoes in the form $Ae^{j\phi} = \Sigma_i A_i e^{j\phi_i}$, where A_i and ϕ_i represents amplitude and phase of the individual components (Argenti et al., 2013). The phase angle ϕ_i varies randomly within the range $(-\pi, \pi)$ because of which echoes interfere constructively or destructively creating positive or negative amplitude peaks. This random variation in amplitude appears as speckle in homogeneous regions even if the underlying target region has same reflectivity. Distribution of amplitude component A in a fully developed speckle with standard deviation σ follows Rayleigh distribution whose probability density function can be represented as (Argenti et al., 2013; Tur et al., 1982),

$$P(A) = \frac{2A}{\sigma} e^{-\frac{A^2}{\sigma}}. \quad (1)$$

SAR image is a representation of mean intensity values of the back scattered echoes where intensity $(I = A^2)$ is the square of amplitude represented by negative exponential distribution. Based on the PDF of intensity values, it can be shown that speckle follows a multiplicative model represented as $U_{(x,y)} = V_{(x,y)} * N_{(x,y)}$, where x and y are the pixel coordinates, U is the noisy image, V the original image and N is the noise component (Goodman, 1976; Tur et al., 1982).

Filtering techniques and noise models used in the early days of SAR despeckling were originally proposed for AWGN. It was common to convert the multiplicative speckle into additive noise to leverage the benefits of existing filters and noise models. Non linear logarithmic transformation alters the statistical properties of speckle, and the model prior to transformation cannot be applied to the log transformed image for denoising. According to Xie et al. (2002), SAR image in intensity

Table 1
Comparison based on Lee's phantom image.

Method	SAR-BM3D			PPB			GGF-SAR			PROPOSED		
L	L1	L2	L3	L1	L2	L3	L1	L2	L3	L1	L2	L3
PSNR	36.98	37.99	37.82	37.01	37.52	38.83	36.54	36.9158	36.64	36.89	38.97	38.83
ENL	113.04	167.72	181.92	101.66	151.01	130.58	124.23	166.10	172.99	127.89	157.48	166.74

Fig. 2. 2-Look horse track image.

format when undergone logarithmic transformation follows Gamma distribution. Images in amplitude format obeys Fisher-Tippet density function (Kaplan and Ma, 1993) and amplitude SAR images which is estimated indirectly as the square root of intensity adheres to χ distribution. High resolution SAR images of urban regions generally comes under the category of non-Rayleigh distributed speckle as discussed in Delignon and Pieczynski (2002). In such SAR images, number of scatterers in the resolution cell can be considered as a random variable which follows Poisson distribution with its mean itself as another random variable. If the mean follows Gamma distribution, then the distribution of resulting intensity image obeys K distribution (Delignon and Pieczynski, 2002). In order to accommodate the impulsive and skewed behavior of speckle distribution, several other models where suggested which includes Weibull, log-normal, α-stable and Generalized (heavy-tailed) Rayleigh distributions. In Kuruoglu and Zerubia (2004), non-Rayleigh speckle models are discussed and it is shown that α-stable distribution can be considered as a generalized case of Rayleigh distribution.

Imaging same target region at different intervals and combining those images together is called multi-looking, which reduces speckle at the cost of spatial resolution. Considering the number of looks L and the multiplicative model by Goodman (1976), recent works in SAR denoising (Deledalle et al., 2009; Ni and Gao, 2016; Zhong et al., 2009), assumes Nakagami-Rayleigh distribution for the amplitude SAR image represented as:

$$P(u|r) = 2\left(\frac{L}{r}\right)^{L}\frac{1}{\Gamma(L)}e^{-\frac{Lu^2}{r}}u^{2L-1} \tag{2}$$

where u is the observed noisy image, r the reflectivity image (square of amplitudes in the observed noisy image) and L is the number of looks.

3. GGF-BNLM

Generalized Guided Filter with Bayesian Non-Local Means (GGF-BNLM) (Ni and Gao, 2016) used an explicit guidance image to derive the prior component of PPB (Deledalle et al., 2009). PPB calculates likelihood and prior component of probability from noisy image alone. In this section, we discuss the concepts of PPB and guided filtering to understand the principle behind GGF-BNLM. Parametric constants used in GGF-BNLM method are discussed along with their impact on the performance. The drawbacks of the method are also pointed out.

3.1. Probabilistic patch-based weights

Noise free intensity value at location x surrounded by a patch Δ_x for a noisy image u is estimated based on the statistical similarity between other patches Δ_y around pixel y in the search window. Similarity is represented in terms of probability as $\Pi_i p(\theta_{x,i} = \theta_{y,i}|u_{x,i}, u_{y,i})$ where $u_{x,i}$ and $u_{y,i}$ represents the i^{th} pixel within their respective patches (Deledalle et al., 2009). θ is an unknown parameter which describes the parametric model. The PPB being iterative method, considers parameters from previous iteration. Similarity probability can be rewritten as $\Pi_i p(\theta_{x,i} = \theta_{y,i}|u_{x,i}, u_{y,i}, \theta^{t-1})$ where θ^{t-1} represents the estimate of θ at $(t-1)^{th}$ iteration (Deledalle et al., 2009). In the absence of any information on $p(u_{x,i}, u_{y,i})$ and on assumption that $p(u_{x,i}, u_{y,i}|\theta_{x,i} = \theta_{x,i})$ is independent of the previous estimate θ, the modified similarity probability is rewritten based on Bayesian framework as (Deledalle et al., 2009):

$$p\left(\theta_{x,i} = \theta_{y,i}|u_{x,i}, u_{y,i}, \theta^{t-1}\right) \propto p\left(u_{x,i}, u_{y,i}|\theta_{x,i} = \theta_{y,i}\right)p\left(\theta_{x,i} = \theta_{y,i}|\theta^{t-1}\right) \tag{3}$$

Prior term $p(\theta_{x,i} = \theta_{y,i}|\theta^{t-1})$ in (3) measures the validity of assumption $\theta_{x,i} = \theta_{y,i}$ given the information about θ^{t-1} in hand. Assuming Nakagami-Rayleigh distribution (Goodman, 1976; Deledalle et al., 2009), for speckle, the distribution of amplitude A can be represented by (4) (similar to (2)), where intensity of the noisy image R serves as the distribution parameter (Deledalle et al., 2009).

$$P(A|R) = 2\left(\frac{L}{R}\right)^{L}\frac{1}{\Gamma(L)}e^{-\frac{LA^2}{R}}A^{2L-1} \tag{4}$$

Likelihood and Prior terms at t^{th} iteration in (3) is then approximated respectively as (Deledalle et al., 2009):

$$p\left(A_{x,i}, A_{y,i}|R_{x,i} = R_{y,i}\right) \propto \left(\frac{A_{x,i}A_{y,i}}{A_{x,i}^2 + A_{y,i}^2}\right)^{2L-1} \tag{5}$$

$$p\left(R_{x,i} = R_{y,i}|R^{t-1}\right) \propto exp\left(-\frac{L}{T}\frac{\left(\left|R_{x,i}^{t-1} - R_{y,i}^{t-1}\right|\right)^2}{R_{x,i}^{t-1}R_{y,i}^{t-1}}\right) \tag{6}$$

Combining likelihood and prior terms, the weight of similarity between patches Δ_x and Δ_y at iteration t is rewritten as (Deledalle et al., 2009):

$$w(x,y) = exp\left[-\sum_k\left(\frac{1}{h}log\left(\frac{A_{x,i}}{A_{y,i}} + \frac{A_{y,i}}{A_{x,i}}\right) + \frac{L}{T}\frac{\left|R_{x,i}^{t-1} - R_{y,i}^{t-1}\right|^2}{R_{x,i}^{t-1}R_{y,i}^{t-1}}\right)\right] \tag{7}$$

here h is the normalization constant. Detailed analysis on the significance of h and its decisive role in controlling the smoothing is discussed in Section 5. T represents the number of iteration and it extends to ∞ until

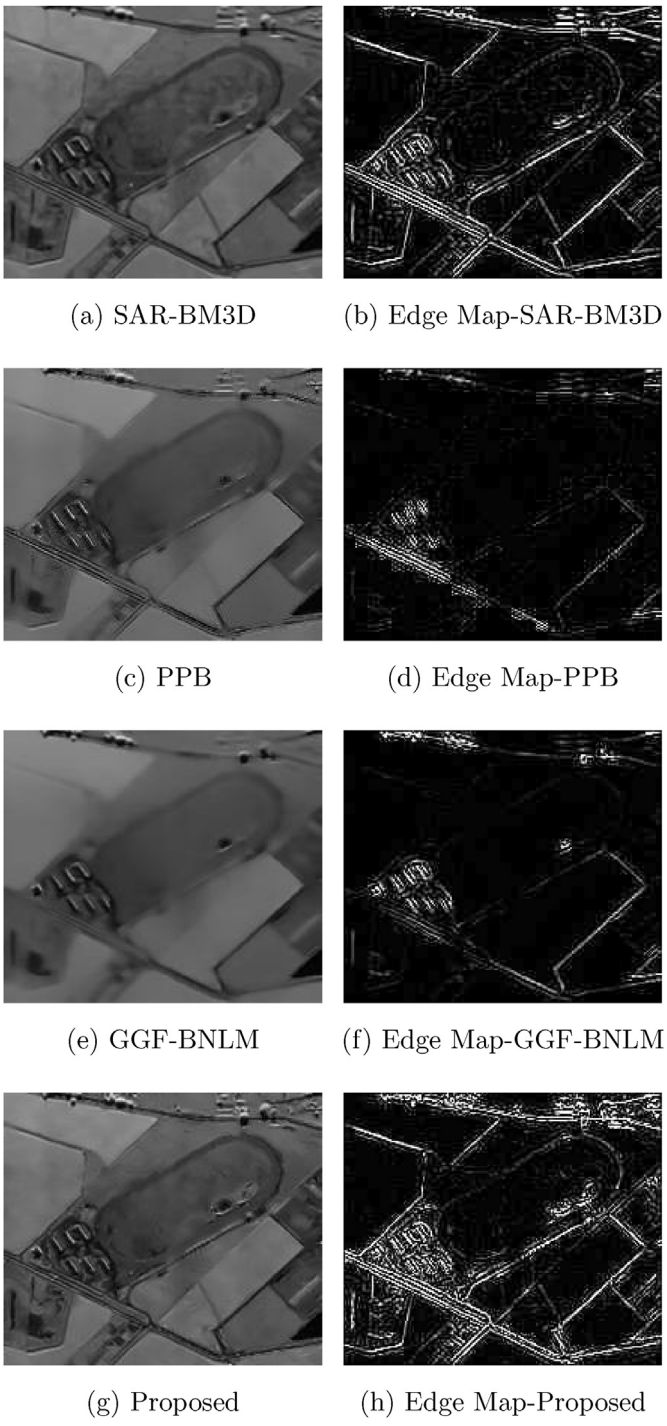

Fig. 3. Filtered outputs and their corresponding edge maps for 1-Look Horse track image.

the required level of convergence is achieved.

3.2. Guided filtering

In Guided Filtering, a linear relationship is assumed between the guidance image g and the denoised output image v. For every window of pixels Δ_x surrounding the pixel x, this linear relationship is represented as $v_i = a_{x,i}g_i + b_x, \forall_i \in \Delta_x$, where a_x and b_x are linear coefficients which are constant for the window Δ_x (He et al., 2013). Weights a_x and b_x which forms the coefficients for linear model are then calculated for each window Δ_x from noisy input u and g by means of linear ridge regression analysis and is expressed as (He et al., 2013; Ni and Gao, 2016),

Table 2
Edge Preservation Factor: Horse Track image.

Method	EPF	ENL
SAR-BM3D	0.3026	197.2627
PPB	0.2777	264.8479
GGF-BNLM	0.2028	326.8252
PROPOSED	0.5371	285.2966

$$a_k = \sum_{i\in\Delta_x} A_{x,i}(g)u_i \tag{8}$$

$$b_k = \sum_{i\in\Delta_x} B_{x,i}(g)u_i \tag{9}$$

The functions $A_{x,i}(g)$ and $B_{x,i}(g)$ depends only on g (Ni and Gao, 2016). In order to solve the problem of multiple estimations for the same pixel v_i under different overlapping windows Δ_x, all the possible values are averaged together using $|\Delta_x|$.

3.3. Generalized guided filter with Bayesian non-local means

GGF-BNLM derives Likelihood from noisy image u and prior assumptions are made from an explicit guidance image g. Substituting the expressions for a_k and b_k given in (8) and (9), in the expression $v_i = a_{x,i}g_i + b_x, \forall_i \in \Delta_x$, the noise free pixel value at location i, v_i can be expressed according to Guided Filter as below (Ni and Gao, 2016):

$$v_i = \frac{1}{|\Delta_x|}\sum_{i\in\Delta_x}\sum_{j\in\Delta_x}\left[A_{x,j}(g_i)g_i + B_{x,j}(g_i)\right]u_j \tag{10}$$

By rearranging the order of summation and considering the symmetric nature of patches, (10) is reduced and rewritten as (He et al., 2013) (Ni and Gao, 2016),

$$v_i = \sum_j W_{i,j}(u,g)u_j \tag{11}$$

where $W_{i,j}(u,g)$ is the weight function $A_{x,j}(g_i)g_i + B_{x,j}(g_i)$. GGF-BNLM used a modified non-linear weight function (Ni and Gao, 2016) that is different from (7) as given below (He et al., 2013)

$$w_{i,j}(u,g) = \exp\left\{-\left[\frac{1}{K_1}\sum_m \log\left(\frac{u_{i,m}^2 + u_{j,m}^2}{u_{i,m}u_{j,m}}\right) + \frac{L}{K_2}\sum_m \frac{\left|\left(g_{i,m}\right)^2 - \left(g_{j,m}\right)^2\right|^2}{\left(g_{i,m}\right)^2\left(g_{j,m}\right)^2}\right]\right\} \tag{12}$$

here, constants K_1 and K_2 determines the relative contribution of likelihood and prior components, u is the noisy input image and g is the guidance image.

3.4. Drawbacks of GGF-BNLM

With the number of looks L and K_2 set to constant values, K_1 determines the relative contribution of likelihood component estimated from u in deriving the exponential weight. Smaller values for K_1 makes the GGF-BNLM similar to that of a Non-Local filter with probabilistic weights. On the other hand with a constant L and K_1, K_2 decides the contribution of prior component from guidance image g in calculating the exponential weights. Values K_1 and K_2 are derived based on heuristics and it can be experimentally shown that one set of values which gives optimal result for an image need not work well for all the other images. K_1 and K_2 are derived from experimental analysis such that the pair which gives optimal values in terms of PSNR and ENL are chosen. GGF-BNLM is found to introduce unwanted swirling artifacts in homogeneous

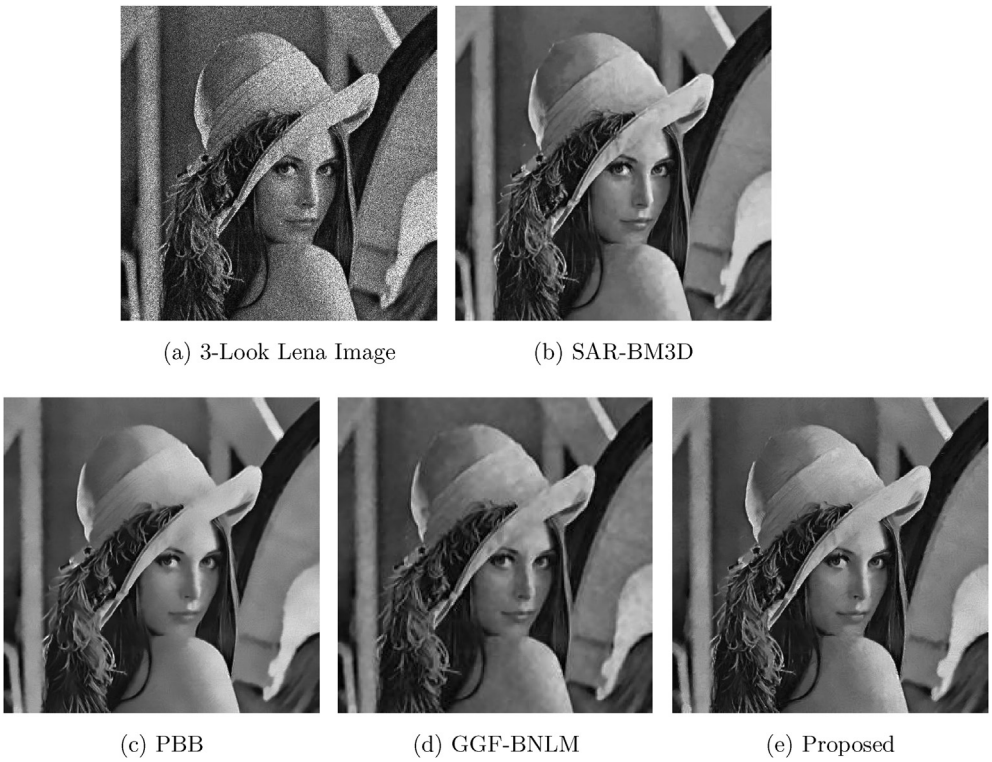

Fig. 4. Comparison of filters for 3-Look Lena image.

Table 3
Performance analysis of the proposed method against SAR-BM3D, PPB and GGF-BNLM.

Method	PSNR	ENL
(a) Lena Image		
SAR-BM3D	34.4661	255.3220
PPB	33.0526	244.9020
GGF-BNLM	33.5673	235.9337
PROPOSED	36.1627	270.2453
(b) House Image		
SAR-BM3D	35.4634	154.1602
PPB	33.0519	396.3305
GGF-BNLM	36.4944	645.9174
PROPOSED	37.8950	695.6984

regions of the filtered output (Ni and Gao, 2016) and this happens because of the high variance in homogeneous regions. Feature preservation in GGF-BNLM is better when compared to PPB, but speckle suppression and smoothing in homogeneous region is compromised in achieving this.

4. Guided SAR despeckling with probabilistic non-local weights

We propose a modified edge preserving SAR despeckling technique, which is based on Guided Filtering in the Bayesian Non-Local framework. The proposed technique use dynamically derived coefficients for likelihood and prior components in the probabilistic weight function, instead of parametric constants based on heuristics in GGF-BNLM. This ensures that the proposed technique gives optimal performance across various SAR images irrespective of the parametric constants used. We also propose an alternative method for more accurate construction of the guidance image, as the prior assumptions about noise distribution is made from the guidance image. The proposed SAR despeckling consists of construction of guidance image, estimation of controlling parameters, weight coefficient for likelihood component and weight coefficient for prior component.

4.1. Coefficients for likelihood and prior components

Parameters K_1 and K_2 given in (12) for GGF-BNLM determines the relative contribution of likelihood and prior components in estimating the noise free pixel values at location i. They decides the degree of smoothing and also controls the role of guidance image g and the noisy image u in weight estimation. In the proposed method, K_1 and K_2 are replaced by statistical measures based on u.

NLM used a parametric constant h, which controls the degree of smoothing. h also influences the decay of exponential weight function (Buades et al., 2005) and is deterministically related to the statistical properties of the image. NLM estimates the value h as the standard deviation of noise in the input image. In PPB, similarity criteria between patches in terms of probability is represented as (Deledalle et al., 2009)

$$w(x,y) \propto exp\left(\frac{1}{h} logp\left(\theta_x = \theta_y | u\right)\right) \tag{13}$$

Parameter h normalizes the similarity criterion and have similar functionality to h used in NLM. The parameter h is approximated as the α-quantile of the normalized similarity criteria between noisy patches Δ_x and Δ_y having identical parameters $\theta_x = \theta_y$, which is calculated as (Deledalle et al., 2009)

$$h = q - E\left[c\left(\Delta_x, \Delta_y\right)\right] \tag{14}$$

here q is the α-quantile of the similarity criteria given by $q = F^{-1}_{c(\Delta_x,\Delta_y)}(\alpha)$ and F is the cumulative distribution function (CDF) of the similarity criteria represented by (Deledalle et al., 2009)

$$c\left(\Delta_x \cdot \Delta_y\right) = -\sum_k \log\left(p\left(u_{x,k}, u_{y,k} | \theta_x = \theta_y\right)\right) \tag{15}$$

We suggest to use the parameter h discussed in PPB in place of the parameter K_1 used in GGF-BNLM as the controlling parameter for likelihood component. This will ensure that the weight estimated from similarity probability is directly related to the range of the similarity

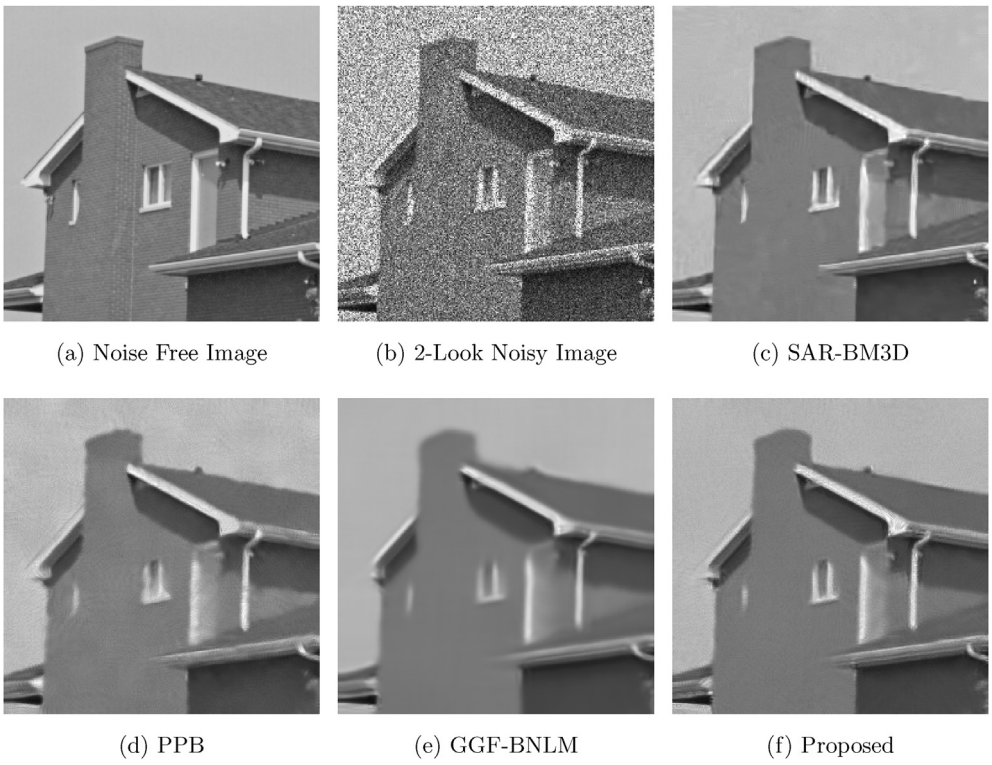

Fig. 5. Comparison of proposed method with the other state-of-the-art filters for House image.

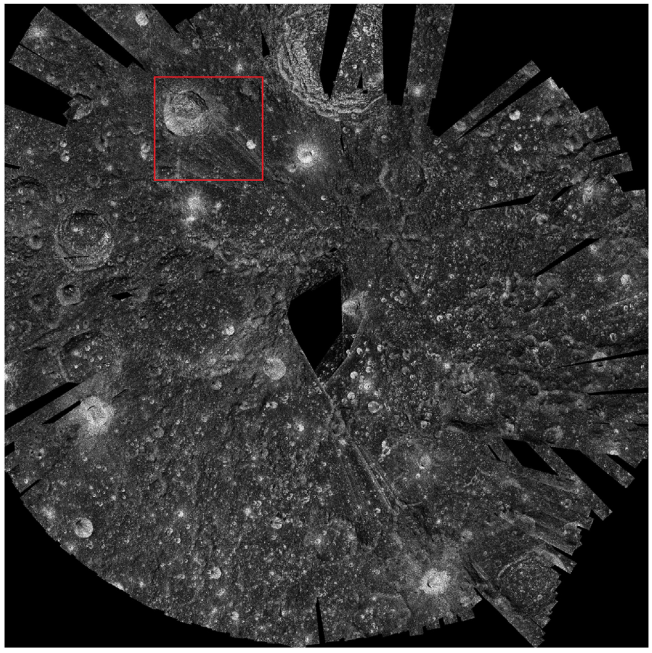

Fig. 6. Original speckled lunar image from CHANDRAYAN-I mission with size 2027 × 2027.

criteria used and will in turn control the degree of smoothing. Considering the number of looks L, the normalization parameter h is then modified as (He et al., 2013):

$$\widehat{h} = \frac{h}{2L-1} \tag{16}$$

We also suggest to use coefficient of variance based on local image statistics as the coefficient for prior component in the exponential weight function given in (12). Prior component is purely assumed from the guidance image and it decides the relative contribution of guidance image in weight calculation. If the relative contribution of guidance image g is minimal, then the entire weight estimation is more aligned to the PPB filtering approach with negligible contribution from guided filtering part. For the estimation of weights $w(i,j)$ for those pixels i inside patches Δ_i having lot of details like edges, prior component is given more weightage, as the guidance image g has more edge information than the noisy input image. Coefficient of variance within patch Δ_i is taken into consideration for determining the coefficient for prior component. Coefficient of variance C_i is represented as (Lee, 1980):

$$C_i = \frac{\sqrt{var(\Delta_i)}}{E[\Delta_i]} \tag{17}$$

where *var* is the variance and E is the expectation of the patch Δ_i.

Rather than having a fixed weight coefficient for prior component, a value based on information richness within the local patch would make the prior component contribute towards weight estimation adaptively. Coefficient of variance is the ratio of standard deviation to mean within the local image patch. With the new weight coefficients for likelihood and prior components as given in (16) and (17), $w_{i,j}(u,g)$ can be rewritten as:

$$w_{i,j}(u,g) = \exp\left\{ -\left[\frac{1}{\widehat{h}}\sum_m \log\left(\frac{u_{i,m}^2 + u_{j,m}^2}{u_{i,m}u_{j,m}}\right) + LC_i \sum_m \frac{\left|\left(g_{i,m}\right)^2 - \left(g_{j,m}\right)^2\right|^2}{\left(g_{i,m}\right)^2\left(g_{j,m}\right)^2}\right]\right\} \tag{18}$$

4.2. Construction of guidance image

Accurate approximation of the guidance image g helps in making better prior assumptions about the noise distribution. GGF-BNLM used

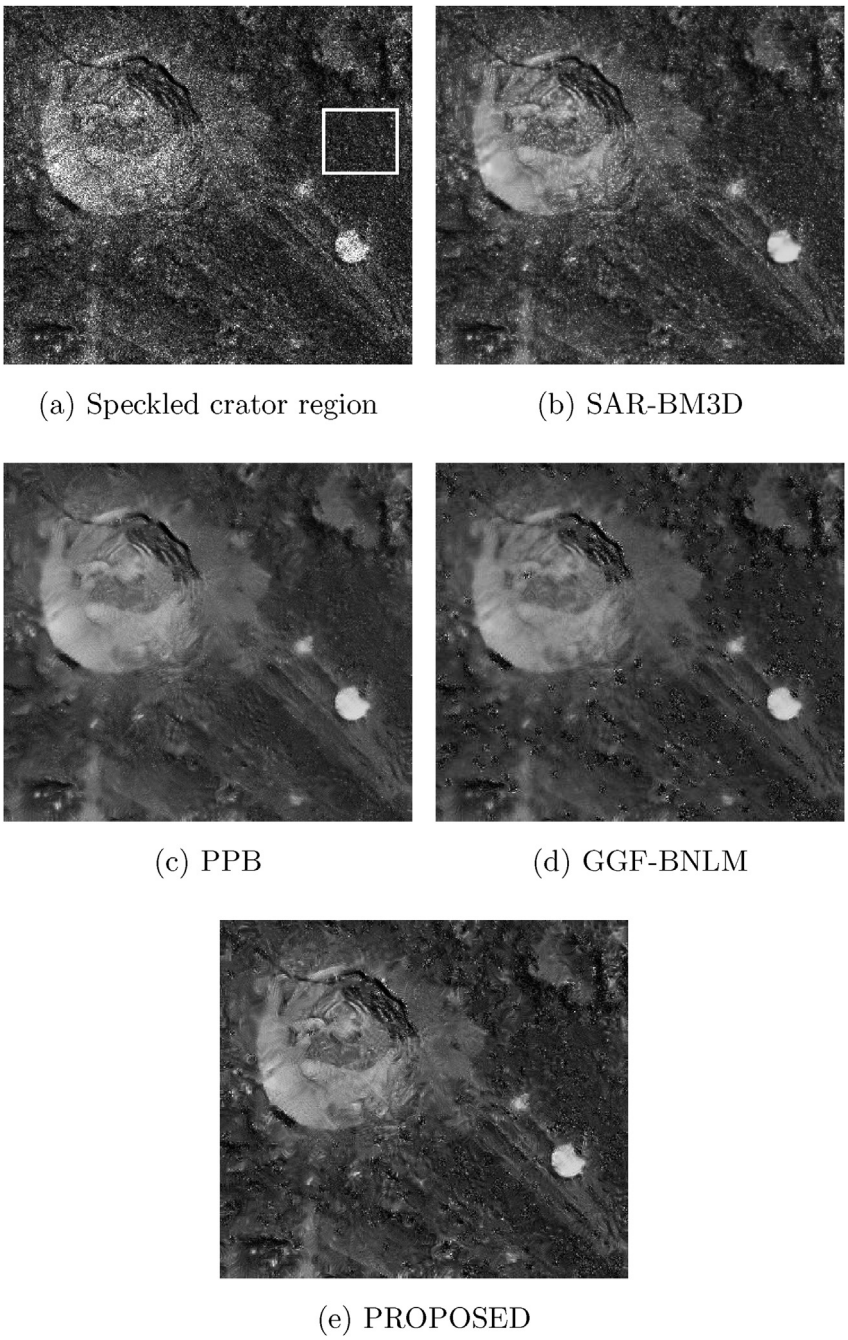

Fig. 7. (a) Cropped CHANDRAYAN-I image. Results for (b) SAR-BM3D [ENL = 21.8425], (c) PPB [ENL = 24.5322], (d) GGF-BNLM [ENL = 26.2100] and (e) Proposed Method [ENL = 29.1174].

region homogeneity analysis for the construction of guidance image, where variance of the pixel is used as measure of region homogeneity. We propose to use a more elegant and simple linear local statistic filter based on MMSE (Lee, 1980) for the construction of guidance image. This helps in construction of a guidance image with more detail being preserved and in turn makes better prior assumptions while calculating the exponential weights. Linear filters which follows MMSE estimation can be represented as (Argenti et al., 2013):

$$v_i = \widehat{u_i} + [u_i - \widehat{u_i}] * w(i) \tag{19}$$

where v_i is the denoised value, u_i and $\widehat{u_i}$ are the noisy pixel and mean of the moving window centered at position i respectively in the noisy input image u. $w(i)$ is a weight function which has value ranging from 0 to 1 depending on the local image statistics. Among the classic adaptive linear filters, Lee filter performs better in terms of edge preservation and hence in our method, we suggest to use the weight function $w(i)$ as discussed in Lee (1980).

$$w(i) = 1 - \frac{C_n^2}{C_I^2(i)} \tag{20}$$

where $C_n = \frac{\sigma_n}{\widehat{I}}$ and $C_I = \frac{\sigma_i}{\widehat{I}_i}$. σ_n is the standard deviation of the entire noisy image and $\widehat{I}$ is its expectation. σ_i is the standard deviation of the local window around pixel i and $\widehat{I}_i$ is the expectation within local window.

5. Experimental results and analysis

In this section, we present the results of the experiments conducted to demonstrate the effectiveness of the proposed SAR despeckling technique. Experiments were conducted on synthetic and real SAR images to illustrate the edge preservation and speckle suppression capabilities of the proposed filter. Results are also compared against some of the popular and state-of-the-art NLM based SAR despeckling techniques which includes PPB (Deledalle et al., 2009), Block Matching 3D filter for SAR despeckling (SAR-BM3D) (Parrilli et al., 2012) and GGF-BNLM (Ni and Gao, 2016). Synthetic images are created by adding multiplicative Goodman speckle (Goodman, 1976) into noise free images.

5.1. Experimental setup

For the experimental analysis, search window and similarity window of the proposed method are chosen as 21×21 and 3×3 respectively. The parameter α for determining the normalization factor h is set to 0.92 as recommended in (Deledalle et al., 2009). In GGF-BNLM, a search window of size 21×21 and similarity window of size 7×7 and parameters K_1 and K_2 are set as 45 and 100 respectively, as recommended in Ni and Gao (2016). For an iterative version of PPB, the default search and similarity windows of size 10×10 and 3×3 are chosen respectively with α set to a value of 0.92 and T is fixed to 0.2 as recommended in Deledalle et al. (2009). In SAR-BM3D, the block size is set to 8 with a search area diameter of 39, step size of sliding window is chosen as 3 and parameter β for 2D Kaiser window is set to 2.0 as mentioned in Parrilli et al. (2012). The above mentioned parameters are used throughout the experimental analysis, unless specified explicitly. Experiments were carried out on a workstation with Intel Xeon E5-2670 v3@2.30 Ghz processor and 128 GB RAM using Matlab R2015a on Windows 10 operating system.

5.2. Evaluation metrics

In order to quantify speckle suppression and feature preservation capabilities, we used - Peak Signal to Noise Ratio (PSNR), and Equivalent Number of Looks (ENL) as the metrics for performance evaluation. Higher the PSNR value, better the results are. ENL indicates the degree of smoothing achieved in homogeneous regions. To evaluate the edge preservation performance in the absence of ground truth, we used a metric called Edge Preservation Factor (EPF) (Sattar et al., 1997). More closer the EPF value is to 1, better the edge preservation is.

5.3. Experimental results for synthetic and real SAR images

Experiment results for phantom image as per Lee's protocol (Moschetti et al., 1788) is given in Fig. 1. ENL is calculated for a rectangular region marked in Fig. 1a. From the experimental results, it is evident that the proposed method is able to strike a balance between speckle suppression and feature preservation and this is backed by the numerical results in Table 1.

In order to analyze the edge preservation capabilities of the proposed filter, experiments were carried out on a 2-Look horse track image shown in Fig. 2. Laplacian operator is then applied on the filtered outputs to identify the salient edges and thereby to demonstrate how well the edges are preserved after filtering. Results of this experiment is shown in Fig. 3 with the quantitative analysis given in Table 2 for comparison. It is evident from Fig. 3h that the proposed method performs well in terms of edge preservation and has produced an EPF value higher than the other methods under consideration. ENL is calculated for region marked by rectangle in Fig. 2. Only GGF-BNLM has higher ENL value than the proposed method for the given image. This is because of the excessive smoothing achieved at the cost of image details.

Experimental results for Lena image is given in Fig. 4. Noise free image is corrupted with 3-Look speckle to form the noisy image and is shown in Fig. 4a. The filtered results for SAR-BM3D, PPB, GGF-BNLM and proposed method are given in Fig. 4b–e respectively. SAR-BM3D is found to retain residuals of speckle in homogeneous regions and this is evident in visual analysis. PPB suppresses the speckle to an extend but lags behind SAR-BM3D in terms of feature preservation. GGF-BNLM on the other hand suffers from excessive smoothing. From the experimental results, it is evident that the proposed method is able to strike a balance between speckle suppression and feature preservation and this is backed by the numerical results in Table 3a for Lena image. Proposed method outperforms other filters in terms of PSNR and ENL due to excellent speckle suppression achieved and also the high degree of smoothing achieved in the homogeneous regions.

Results of the experiments carried out on a noise free House image (Fig. 5a) corrupted with 3-Look speckle (Fig. 5b) is given in subsequent sub figures of Fig. 5. Quantitative analysis in terms of PSNR and ENL is given in Table 3b.

The proposed method was also tested on real speckled lunar SAR images collected from Chandrayan-I mission. Chandrayan-I is an active remote sensing lunar probe launched in October 2008 by Indian Space Research Organisation, which pictured the polar regions of the moon using an active SAR system which operated in 2.5 GHz frequency. The original 2027×2027 lunar image corrupted with speckle is shown in Fig. 6. For better visual inspection, only a zoomed in region (marked by red rectangle in Fig. 6) is presented in Fig. 7 as the outputs from various filters. ENL is calculated for the region marked by rectangle in Fig. 7a. Proposed method gave highest ENL value for the marked region, in comparison with other techniques.

5.4. Computational complexity

Computational complexities of SAR-BM3D, PPB, GGF-BNLM and the proposed method are asymptotically analyzed and compared in this section. All of the above listed techniques fits into the category of non local filtering and hence, the computational cost depends on size of the image (I), search window (W) and similarity window (S). PPB is an iterative approach which iteratively refines the probabilistic weights for T iterations and hence, its complexity is of the order of $O(T{*}IWS)$. Complexity of SAR-BM3D is of the order of $O(IWS + IW)$ (Ni and Gao, 2016). GGF-BNLM has a complexity of $O(IWS + IS)$. In the proposed method, the coefficient of likelihood is calculated only once based on the α-quantile of the noisy input. Coefficient of variance C_v is calculated once for each window W and hence the complexity of the proposed method is of the order of $O(IW + IWS)$. Search window and similarity window being negligible when compared with size of image, complexity predominantly depends on I, the image size.

6. Conclusion

Despeckling of SAR images is an active area of research with several new methods being proposed every year. Two highly desired qualities of despeckled SAR images are high level of speckle suppression and excellent feature preservation. Most of the techniques proposed so far, achieves speckle suppression by over smoothing and while doing so, important features are lost. In order to bridge this gap, an improved SAR despeckling technique based on guided filtering in the Bayesian non-local framework was proposed which achieves smoothing, without compromising feature preservation. Normalization coefficients for likelihood and prior components were adaptively derived from the image statistics itself, unlike the earlier guided SAR despeckling techniques which determined the coefficients based on heuristics. In order to improve the prior assumption on the noise distribution, we used simple and more efficient linear filter based on MMSE estimation for creating the guidance image. Experiments were carried out on both synthetic and real SAR images to evaluate the performance of the proposed method. Results were compared with other state-of-the-art SAR despeckling filters in the NLM framework which includes PPB, SAR-BM3D and GGF-BNLM. On

experimental analysis, the proposed method gave better results for speckle suppression with high degree of smoothing achieved in homogeneous regions. Edge and feature preservation capabilities of the proposed method were found to be effective in comparison with the other filters.

Acknowledgment

The authors would like to thank J. D. Rao, Deputy General Manager, Indian Space Science Data Centre, ISTRAC for providing CHANDRAYAN-I images.

References

Argenti, F., Lapini, A., Bianchi, T., Alparone, L., 2013. A tutorial on speckle reduction in synthetic aperture radar images. IEEE Geosci. Remote Sens. Mag. 1 (3), 6–35.

Bianchi, T., Argenti, F., Alparone, L., 2008. Segmentation-based map despeckling of sar images in the undecimated wavelet domain. IEEE Trans. Geosci. Remote Sens. 46 (9), 2728–2742.

Buades, A., Coll, B., Morel, J.M., 2005. A non-local algorithm for image denoising. In: Computer Vision and Pattern Recognition, 2005. CVPR 2005. IEEE Computer Society Conference on, vol. 2, pp. 60–65.

Coupe, P., Hellier, P., Kervrann, C., Barillot, C., 2008. Bayesian non local means-based speckle filtering. In: Biomedical Imaging: from Nano to Macro, 2008. ISBI 2008. 5th IEEE International Symposium on, pp. 1291–1294.

Deledalle, C.A., Denis, L., Tupin, F., 2009. Iterative weighted maximum likelihood denoising with probabilistic patch-based weights. IEEE Trans. Image Process. 18 (12), 2661–2672.

Delignon, Y., Pieczynski, W., 2002. Modeling non-rayleigh speckle distribution in sar images. IEEE Trans. Geosci. Remote Sens. 40 (6), 1430–1435.

Frost, V.S., Stiles, J.A., Shanmugan, K.S., Holtzman, J.C., 1982. A model for radar images and its application to adaptive digital filtering of multiplicative noise. IEEE Trans. Pattern Anal. Mach. Intell. PAMI 4 (2), 157–166.

Goodman, J.W., 1976. Some fundamental properties of speckle. J. Opt. Soc. Am. 66 (11), 1145–1150. http://www.osapublishing.org/abstract.cfm?URI=josa-66-11-1145.

He, K., Sun, J., Tang, X., 2013. Guided image filtering. IEEE Trans. Pattern Anal. Mach. Intell. 35 (6), 1397–1409.

Jojy, C., Nair, M.S., Subrahmanyam, G.R.K.S., R, R., 2013. Discontinuity adaptive non-local means with importance sampling unscented kalman filter for de-speckling sar images. IEEE J. Sel. Top. Appl. Earth Obs. Remote Sens. 6 (4), 1964–1970.

Kaplan, D., Ma, Q., 1993. On the statistical characteristics of log-compressed rayleigh signals: theoretical formulation and experimental results. In: Ultrasonics Symposium, 1993. Proceedings., IEEE 1993, vol. 2, pp. 961–964.

Kuan, D.T., Sawchuk, A.A., Strand, T.C., Chavel, P., 1985. Adaptive noise smoothing filter for images with signal-dependent noise. IEEE Trans. Pattern Anal. Mach. Intell. PAMI 7 (2), 165–177.

Kuruoglu, E.E., Zerubia, J., 2004. Modeling sar images with a generalization of the rayleigh distribution. IEEE Trans. Image Process. 13 (4), 527–533.

Lee, J.S., 1980. Digital image enhancement and noise filtering by use of local statistics. IEEE Trans. Pattern Anal. Mach. Intell. PAMI 2 (2), 165–168.

Lopes, A., Nezry, E., Touzi, R., Laur, H., 1990. Maximum a posteriori speckle filtering and first order texture models in sar images. In: Geoscience and Remote Sensing Symposium, 1990. IGARSS '90. 'Remote Sensing Science for the Nineties'., 10th Annual International, pp. 2409–2412.

Lopes, A., Touzi, R., Nezry, E., 1990. Adaptive speckle filters and scene heterogeneity. IEEE Trans. Geosci. Remote Sens. 28 (6), 992–1000.

Moreira, A., Prats-Iraola, P., Younis, M., Krieger, G., Hajnsek, I., Papathanassiou, K.P., 2013. A tutorial on synthetic aperture radar. IEEE Geosci. Remote Sens. Mag. 1 (1), 6–43.

Moschetti, E.E., Palacio, G., Picco, M., Bustos, O.H., Frery, A.C., 1788. On the Use of Lee's Protocol for Speckle-reducing Techniques, CoRR abs/1209. http://arxiv.org/abs/1209.1788.

Ni, W., Gao, X., 2016. Despeckling of sar image using generalized guided filter with bayesian nonlocal means. IEEE Trans. Geosci. Remote Sens. 54 (1), 567–579.

Parrilli, S., Poderico, M., Angelino, C.V., Verdoliva, L., 2012. A nonlocal sar image denoising algorithm based on llmmse wavelet shrinkage. IEEE Trans. Geosci. Remote Sens. 50 (2), 606–616.

Sattar, F., Floreby, L., Salomonsson, G., Lovstrom, B., 1997. Image enhancement based on a nonlinear multiscale method. IEEE Trans. Image Process. 6 (6), 888–895.

Tao, R., Wan, H., Wang, Y., 2012. Artifact-free despeckling of sar images using contourlet. IEEE Geosci. Remote Sens. Lett. 9 (5), 980–984.

Tur, M., Chin, K.C., Goodman, J.W., 1982. When is speckle noise multiplicative? Appl. Opt. 21 (7), 1157–1159. http://ao.osa.org/abstract.cfm?URI=ao-21-7-1157.

Verdoliva, L., Amitrano, D., Gaetano, R., Ruello, G., Poggi, G., 2014. Sar despeckling guided by an optical image. In: Geoscience and Remote Sensing Symposium (IGARSS), 2014 IEEE International, pp. 3698–3701.

Verdoliva, L., Gaetano, R., Ruello, G., Poggi, G., 2015. Optical-driven nonlocal sar despeckling. IEEE Geosci. Remote Sens. Lett. 12 (2), 314–318.

Xie, H., Pierce, L.E., Ulaby, F.T., 2002. Statistical properties of logarithmically transformed speckle. IEEE Trans. Geosci. Remote Sens. 40 (3), 721–727.

Zhong, H., Li, Y., Jiao, L., 2009. Bayesian nonlocal means filter for sar image despeckling. In: Synthetic Aperture Radar, 2009. APSAR 2009. 2nd Asian-Pacific Conference on, pp. 1096–1099.